NASA
Technical Memorandum 81532

AVRADCOM
Technical Report 80-C-15

LOSS MODEL FOR OFF-DESIGN PERFORMANCE ANALYSIS OF RADIAL TURBINES WITH PIVOTING-VANE, VARIABLE-AREA STATORS

Peter L. Meitner
Propulsion Laboratory
AVRADCOM Research and Technology Laboratories
Lewis Research Center

and

Arthur J. Glassman
Lewis Research Center
Cleveland, Ohio

Prepared for the
Aerospace Congress
sponsored by the Society of Automotive Engineers
Los Angeles, California, October 13-16, 1980

NASA

LOSS MODEL FOR OFF-DESIGN PERFORMANCE ANALYSIS OF RADIAL TURBINES WITH PIVOTING-VANE, VARIABLE-AREA STATORS

by Peter L. Meitner
Propulsion Laboratory
AVRADCOM Research and
Technology Laboratories
Lewis Research Center

and

Arthur J. Glassman
Lewis Research Center
Cleveland, Ohio

ABSTRACT

An off-design performance loss model is developed for variable-area (pivoted vane) radial turbines. The variation in stator loss with stator area is determined by a viscous loss model while the variation in rotor loss due to stator area variation (for no stator end-clearance gap) is determined through analytical matching of experimental data. An incidence loss model is also based on matching of the experimental data. A stator vane end-clearance leakage model is developed and sample calculations are made to show the predicted effects of stator vane end-clearance leakage on performance.

FOR AUTOMOTIVE OR HELICOPTER APPLICATIONS gas turbine engine must operate over a wide range of power settings. Conventional engine throttling (part power operation) is achieved by reducing engine speed, and therefore cycle pressure ratio, and temperature, which reduces overall thermal efficiency. To reduce engine thermal efficiency loss at part power, it is desirable to maintain constant engine speed, pressure ratio and temperature, while throttling with internal area changes to reduce flow, and thus power. A radial turbine with variable area stators can be operated in this manner over a broad flow range, and if high turbine efficiency can be maintained, it can contribute significantly to high engine performance at part power. However, the effect of stator area variation and stator end-clearance leakage on turbine performance must be known for proper engine performance prediction.

This paper presents a loss model for the off-design performance prediction of radial turbines with pivoted vane, variable-area stators. The model is based on a previous loss model (1)* which considers stator, incidence, and rotor losses, but which does not consider their variations with stator area changes. In the loss model presented herein, the effect of stator area variation on stator loss is accounted for by a viscous loss model, while the effects on rotor loss (for no stator end-clearance gap) are obtained by analytical matching of experimental data. The experimental data is also used to obtain a revised incidence loss model. Finally, a clearance flow model is proposed to account for the effects of stator vane end-clearance leakage. Sample calculations are made to show the predicted effects of stator end-clearance leakage on performance for this model.

SYMBOLS

A	area, m^2	
AR	stator-to-rotor throat area ratio	
B	blockage factor at stator exit, ratio of area inside blade passage to area outside blade passage	Meitner
C	modifier, set equal to 1.0	
c	stator vane total clearance, m	2
$\bar{e}$	kinetic energy loss coefficient	

*Numbers in parentheses designate References at end of paper.

h	stator vane passage height from hub to shroud, m
i	incidence angle, degrees (defined by Eq. (17))
K	rotor loss coefficient
L	kinetic energy loss, J/kg
l	surface length, m
n	incidence exponent
PR	stator total-pressure ratio (defined by Eq. (2))
P	absolute pressure, N/m^2
Q	volume flow rate, m^3/sec or critical velocity ratio function (defined by Eq. (7))
r	radius, m
Re	Reynolds number based on stator vane chord
s	blade spacing at blade row exit, m
t	trailing edge thickness, m
V	absolute velocity, m/s
W	relative velocity, m/s
w	mass flow rate, kg/s
α	fluid absolute flow angle measured from radial direction at stations 0, 1, 2, and 3 and from axial direction at stations 4 and 5, deg
β	fluid relative flow angle measured from radial direction at stations 0, 1, 2, and 3 and from axial direction at stations 4 and 5, deg
γ	ratio of specific heats
θ	momentum thickness, m
ρ	density, kg/m^3

Subscripts:

c	clearance
IN	incidence
opt	optimum
p	main passage
R	rotor
r	radial component
ref	reference
t	total
u	tangential component
0	station at turbine inlet
1	station immediately upstream of stator exit
2	station immediately downstream of stator exit
2D	two-dimensional
3	station immediately upstream of rotor inlet
3D	three-dimensional
4	station immediately upstream of rotor exit

LOSS MODEL

Figure 1 shows a cross-section of a typical radial turbine and indicates the flow stations pertinent to the loss model description. The loss model presented herein is based on the loss model of (1), in which radial turbine performance is modeled by stator, rotor and incidence losses. This model is modified to account for the effects of stator area variation, and vane end-clearance leakage. In addition, the incidence loss model is changed for better agreement with test data.

STATOR LOSS - The stator loss model considers the vane passage flow, the clearance flow, and the mixing process, which also includes the sudden increase in flow area at the trailing edge.

Passage Flow - The stator passage region is defined as the region between the vanes and extending the height (h - c) of the vanes. Since the vane exit angle can be assumed from the turbine geometry, the vane passage flow rate is

$$w_p = 2\pi r_1 (h - c) B \rho_1 V_1 \cos \alpha_{1,p} \qquad (1)$$

The stator passage loss from station 0 to 1 is represented by a total pressure ratio PR where

$$PR = \frac{p_{1,t}}{p_{0,t}} \qquad (2)$$

The change in stator pressure ratio with stator setting angle is obtained by expressing stator pressure ratio in terms of the kinetic energy loss coefficient $\bar{e}_{3D}$

$$PR = \left[\frac{1 - \bar{e}_{3D} - Q_1}{(1 - \bar{e}_{3D})(1 - Q_1)} \right]^{\gamma/\gamma-1} \qquad (3)$$

and evaluating $\bar{e}_{3D}$ from the viscous loss equation of (2)

$$\bar{e}_{3D} = \frac{EC \left(\frac{\Theta_t}{\ell}\right)_{ref} \left(\frac{Re}{Re_{ref}}\right)^{-0.2} \left(\frac{\ell}{s}\right) \left(\frac{A_{3D}}{A_{2D}}\right)}{\cos \alpha_1 - \frac{t}{s} - HC \left(\frac{\Theta_t}{\ell}\right)_{ref} \left(\frac{Re}{Re_{ref}}\right)^{-0.2} \left(\frac{\ell}{s}\right)} \qquad (4)$$

Meitner

4

where

$$E = \frac{2\left(\frac{1}{1.92} + \frac{Q}{3.2} + \frac{Q^2}{4.8} + \frac{Q^3}{6.72}\right)}{\frac{1}{1.68} + \frac{Q}{2.88} + \frac{Q^2}{4.4} + \frac{Q^3}{6.24}} \quad (5)$$

$$H = \frac{\frac{1}{1.2} + \frac{3Q}{1.6} + \frac{5Q^2}{2.0} + \frac{7Q^3}{2.4} + \frac{9Q^4}{2.8}}{\frac{1}{1.68} + \frac{Q}{2.88} + \frac{Q^2}{4.4} + \frac{Q^3}{6.24}} \quad (6)$$

$$Q = \left(\frac{\gamma - 1}{\gamma + 1}\right)\left(\frac{V}{V_{cr}}\right)^2 \quad (7)$$

$$\left(\frac{\theta_t}{\ell Re^{-0.2}}\right)_{ref} = 0.03734 \quad (8)$$

Clearance Flow - In the absence of experimental data, a clearance flow model is proposed to account for stator end-clearance leakage effects. The clearance flow region is defined as that region extending from the ends of the stator vanes to the passage endwalls (hub and/or tip). It is the area unblocked by vanes, extending over the clearance height, c. This clearance flow model, which predicts effects on performance similar to those found in (3) for an axial turbine with pivoted stator vanes, is based on the following assumptions:

(1) The clearance flow expands to the same stator-exit static pressure as the vane passage flow.

(2) The clearance flow has the same total pressure loss as the vane passage flow.

(3) Stator inlet moment of tangential momentum is conserved in the clearance flow.

From these assumptions, the velocities and densities must be the same for both the passage and clearance flows, but the flow angles will differ. The clearance-flow exit angle is determined from conservation of moment of tangential momentum.

$$\alpha_{1,c} = \sin^{-1}\left[\frac{(rV_u)_0}{(rV)_1}\right] \quad (9)$$

Meitner

Thus, the clearance flow rate is

$$w_c = 2\pi r_1 c \rho_1 V_1 \cos \alpha_{1,c} \quad (10)$$

Mixing - The assumed mixing process that takes place between stations 1 and 2 includes the mixing of the passage and

clearance flows, as well as the expansion of the mixed flow as it fills the space behind the vane trailing edges. The expansion behind the trailing edges takes place even with no clearance flow. Mixing is assumed to occur at constant static pressure with tangential momentum being conserved.

For the mixing process, the total flow is the sum of the passage and clearance flows

$$w = w_p + w_c \tag{11}$$

Conservation of tangential momentum between stations 1 and 2 yields

$$V_{u,2} = \frac{V_1}{w} (w_p \sin \alpha_{1,p} + w_c \sin \alpha_{1,c}) \tag{12}$$

The continuity equation

$$\rho_2 V_{r,2} = \frac{w}{2\pi r_2 h} \tag{13}$$

is solved iteratively with Eq. (12) for $V_{r,2}$ to complete definition of the mixed flow at station 2.

ROTOR LOSS - In the loss model of (1), the rotor loss is calculated by

$$L_R = K \left(\frac{w_3^2 \cos^2 i_3 + w_4^2}{2} \right) \tag{14}$$

The rotor loss L_R represents all losses in the rotor except incidence loss. A variation in rotor loss coefficient K with stator area change is expected because of changes in rotor reaction. That variation was obtained by using the off-design performance computer program of (1) to determine values of rotor loss coefficient that caused calculated total efficiency to match the data of (4).

In (4), a design rotor and two modified rotors (Fig. 2), one with exducer extended to reduce rotor exit area to 53 percent of design area and one with the exducer cut back to increase rotor exit area to 137 percent of design area, were investigated with stators having throat areas of 144, 125, 100, 66, 42, and 20 percent of the design value. All stators were fixed and, thus, had no vane end-clearance leakage. Each configuration used the same vane profile, but had varying numbers of vanes and setting angles to achieve the desired flow areas. The number of vanes and angles for each configuration are shown in Table I. All experiments were conducted at equivalent design

speed over a range of pressure ratios. The data for the design rotor was used to determine the variation in rotor loss coefficient K with stator area. The data for the extended and cutback rotors was used to test the developed correlation.

For each stator tested with the design rotor, turbine efficiency at zero incidence angle (with respect to optimum rotor inlet flow angle) was calculated by the computer program of (1) over a range of rotor loss coefficients, until the calculated total efficiencies best matched the experimental data. The relative loss coefficients (loss coefficients divided by loss coefficient for 144 percent stator area, equal to 0.180) associated with the match points are shown in Fig. 3, plotted against stator-to-rotor throat area ratio, which is selected as the correlating parameter because it reflects changes in turbine reaction and can be evaluated directly from turbine geometry. The stator-to-rotor throat area ratio AR is defined by

$$AR = \frac{A_1 \cos \alpha_1}{A_4 \cos \beta_4} \qquad (15)$$

As seen from Fig. 3, rotor loss coefficient remains constant for area ratios above about 0.6. As area ratio decreases below 0.5, rotor loss coefficient increases rapidly. This trend appears consistent with calculated rotor flow characteristics. Velocity calculations for the turbine hub section (4) show significant flow accelerations across the rotor for stator areas above the design value (AR values above approximately 0.5). As stator area decreases below the design value (AR values below approximately 0.5), increasing flow deceleration takes place. A more detailed description of the analytical data matching is found in (5).

INCIDENCE LOSS - In the loss model of (1), the incidence loss is expressed as

$$L_{IN} = \frac{W_3^2 \sin^n i_3}{2} \qquad (16)$$

where the exponent n is 2 for negative incidence and 3 for positive incidence. The incidence angle is defined with reference to the optimum rotor-inlet flow angle.

$$i_3 = \beta_3 - \beta_{3,opt} \qquad (17)$$

Examination of the experimental performance maps (1) used to derive the incidence loss exponents showed a very limited amount of data in the negative incidence region. The experimental results being analyzed herein (4) provided a much better data base, both in amount of data and range of incidence angle, for modeling incidence loss. In order to obtain a continuous variation in incidence loss with exponent n at negative incidence angles, the equation for incidence loss used herein was changed to that used in (6).

$$L_{IN} = \frac{W_3^2 \left(1 - \cos^n i_3\right)}{2} \qquad (18)$$

The best overall match between analysis and experiment, based on all six stators with the design rotor, was obtained with an exponent n of 2.5 for negative incidence and 1.75 for positive incidence. The modified incidence loss model provided as good an analytical match of the data base in (1) as did the original incidence model.

LOSS MODEL EVALUATION

In this section, calculated turbine overall performance using the developed loss model is compared with the experimental performance data for the design rotor and the modified rotors of (4). Also, the effects of stator vane end-clearance as calculated by the proposed loss model are presented.

DESIGN ROTOR - The experimental data for the design rotor with the six stators (144, 125, 100, 66, 42, and 20 percent design throat area) were used as the data base for the variation in rotor loss coefficient with stator area, as well as for the modified incidence loss model. Figures 4 and 5 show the comparisons between experimental and calculated flow and total efficiency, respectively, at constant design speed, as well as the zero incidence match points. Overall agreement between analysis and experiment is good, with the exception of the 20 percent stator area case. For the 20 percent area case, the velocity calculations of (4) show extensive hub flow separation, which could result in the analysis not matching the trend of the efficiency data.

Figure 6 shows the effect of incorporating the variation in rotor loss coefficient with stator area into the loss model. The solid lines are the design rotor total efficiency predictions using rotor losses

obtained from Fig. 3, while the dashed lines show the predictions using the loss model of (1) (rotor loss kept constant at design point value). The rotor loss variation of Fig. 3 is seen to significantly improve the total efficiency predictions.

MODIFIED ROTORS - The experimental tests of (4) were also conducted with a cutback rotor exducer and an extended rotor exducer having throat areas equal to 137 and 53 percent, respectively, of the design rotor. The cutback rotor was tested with stators corresponding to 144, 125, and 100 percent of the design stator throat area, and the extended rotor was tested with stators corresponding to 100, 66, 42, and 20 percent of the design stator throat area.

The developed loss model was used to predict the results of the cutback and extended rotor tests. The loss coefficients used for the predictic were obtained from Fig. 3. Figures 7 and 8 show the comparison between experimental and calculated flow and total efficiency, respectively, for the cutback and extended rotors. Agreement is generally satisfactory with regard to both level and trend. For the same reasons as discussed for the design rotor, the experimental and analytical efficiency trends for the 20 percent stator do not match as well as for the other stators. The overall agreement, however, sustantiates the validity of the derived correlation of rotor loss coefficient with stator-to-rotor throat area ratio.

STATOR CLEARANCE - All data of (4) were taken with fixed stators having no vane end-clearance and a direct comparison between analytical and experimental results for stator end-clearance leakage is thus not possible. The described clearance flow model was used to predict turbine performance for the design rotor with various stator vane end-clearances. For all calculations with stator vane end-clearance, the stator total pressure ratio PR and the rotor loss coefficient K were assumed to be equal to the no clearance values.

Figure 9 shows the calculated effect of stator clearance on mass flow at constant turbine pressure ratio over a range of stator area. These results are independent of turbine pressure ratio. For a given stator clearance, the mass flow ratio increases rapidly with decreasing stator area. This occurs because the clearance flow becomes a larger portion of the total flow as the passage area decreases. As stator clearance

is increased at a fixed stator area, the mass flow increases at a rate nearly linear with clearance. Figure 10 shows the calculated effect of stator clearance on total efficiency at constant turbine pressure ratio over a range of stator area. These results vary only slightly with turbine pressure ratio. For a given stator clearance, the efficiency penalty due to the clearance flow becomes significantly larger as stator area decreases. This occurs primarily as a result of the greater loss in tangential momentum as clearance flow becomes a larger part of the total flow. As stator clearance is increased at a fixed stator area, the efficiency penalty increases at a rate nearly linear with clearance.

SUMMARY

An off-design performance loss model for a radial turbine with pivoting, variable-area stators was developed through a combination of analytical modeling and analysis of experimental data. A viscous loss model is used for the variation in stator loss with setting angle. Stator vane end-clearance leakage effects are predicted by a clearance flow model. The variation in rotor loss coefficient with stator setting angle (for no stator clearance) is obtained by analytical matching of experimental data for a rotor previously tested (at constant speed) with six stators having throat areas from 20 to 144 percent of design area. An incidence loss model is selected to obtain best agreement with experimental data. Predicted turbine performance is compared with experimental results for the design rotor as well as for versions of the rotor having extended and cutback exducers. Sample calculations are made to show the effects of stator vane end-clearance leakage.

The six design rotor loss coefficients obtained by analysis from the experimental data yield a smooth curve when plotted against stator-to-rotor throat area ratio. For area ratio above 0.6, rotor loss coefficient remains constant. As area ratio decreases below 0.5, rotor loss coefficient increases rapidly. This variation in rotor loss coefficient with stator throat area is consistent with calculated rotor internal flow characteristics.

Predicted flows and total efficiencies for the design rotor, as well as for the rotor with an extended exducer (53 percent

of design rotor throat area) and a cutback exducer (137 percent of design rotor throat area) agree well with experimental results, except for the 20 percent stator area cases, where analysis indicates extensive flow separation. This good agreement substantiates the validity of the derived correlation of rotor loss coefficient with stator-to-rotor throat area ratio.

The stator vane end-clearance leakage model predicts increasing mass flow and decreasing efficiency as a result of end-clearances. These changes become significantly larger with decreasing stator area and vary almost linearly with clearance.

REFERENCES

1. C. A. Wasserbauer and A. J. Glassman, "FORTRAN Program for Predicting Off-Design Performance of Radial-Inflow Turbines," NASA TN D-8063, 1975.

2. A. J. Glassman, "Computer Program for Design Analysis of Radial-Inflow Turbines," NASA TN D-8164, 1976.

3. M. G. Kofskey and K. L. McLallin, "Cold Air Performance of Free Power Turbine Designed for 112-Kilowatt Automotive Gas-Turbine Engine, 3: Effect of Stator Vane End Clearances on Performance." DOE/NASA/1011-78/29, NASA TM-78956, 1978.

4. M. G. Kofskey and W. J. Nusbaum, "Effects of Specific Speed on Experimental Performance of a Radial-Inflow Turbine," NASA TN D-6605, 1972.

5. P. L. Meitner and A. J. Glassman, "Off-Design Performance Loss Model for Radial Turbines with Pivoting Variable-Area Stators." NASA TP-1708, 1980.

6. R. J. Roelke, "Miscellaneous Losses. "Turbine Design and Application, A. J. Glassman, ed., NASA SP-290, Vol. 2, 1973, pp. 125-148.

Table I. - Summary of Geometric Data for

Design, Extended and C ..-Back Rotors

Design Rotor Configurations

Stator throat area (percent design)	No. of stator vanes	Stator exit flow angle- α_1, deg	Rotor exit flow angle- β_4, deg
144	13	64.70	-56.86
125	13	68.00	
100	13	72.47	
66	15	77.75	
42	17	81.38	
20	17	85.00	

Extended Rotor Configurations

Stator throat area (percent design)	No. of stator vanes	Stator exit flow angle- α_1, deg	Rotor exit flow angle- β_4, deg
100	13	72.47	-72.56
66	15	77.75	
42	17	81.38	
20	17	85.00	

Cut-Back Rotor Configurations

Stator throat area (percent design)	No. of stator vanes	Stator exit flow angle- α_1, deg	Rotor exit flow angle- β_4, deg
144	13	64.70	-42.07
125	13	68.00	
100	13	72.47	

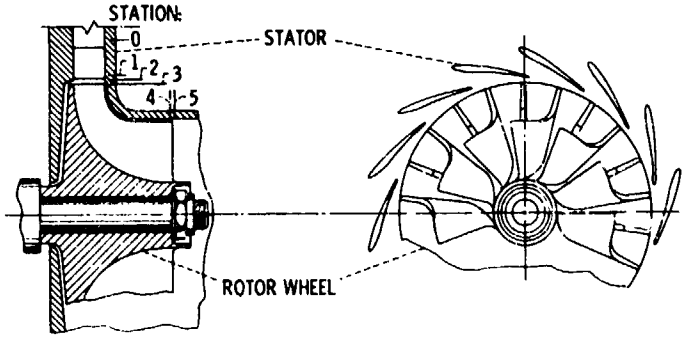

Figure 1. - Cross section of radial turbine.

CD-11857-02

C-71-759

(a) DESIGN ROTOR.

C-69-1816

(b) ROTOR WITH EXDUCER EXTENSION.

C-70-3533

(c) CUTBACK ROTOR.

Figure 2. Rotor configurations.

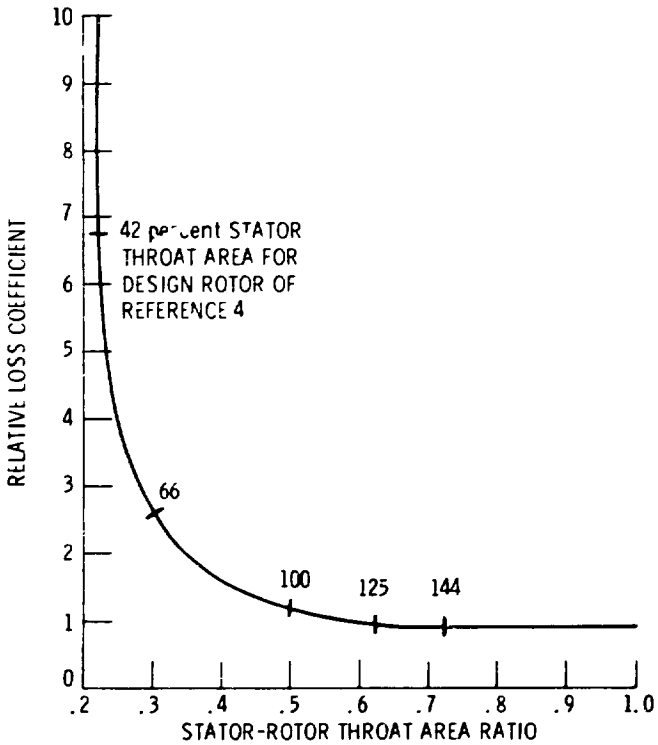

Figure 3. - Rotor relative loss coefficient vs. stator-rotor throat area ratio.

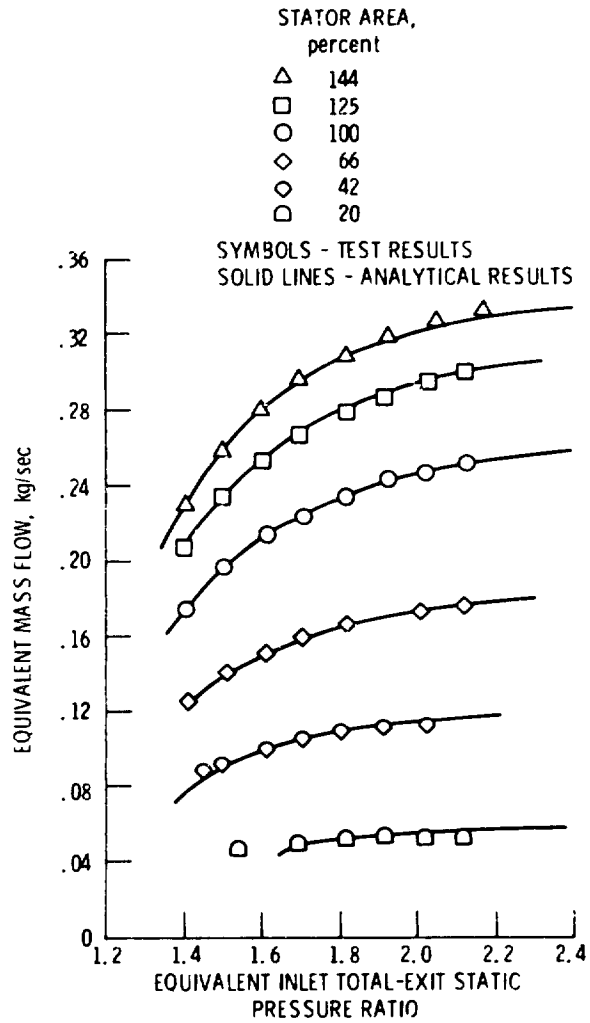

Figure 4. - Design rotor mass flow vs. pressure ratio.

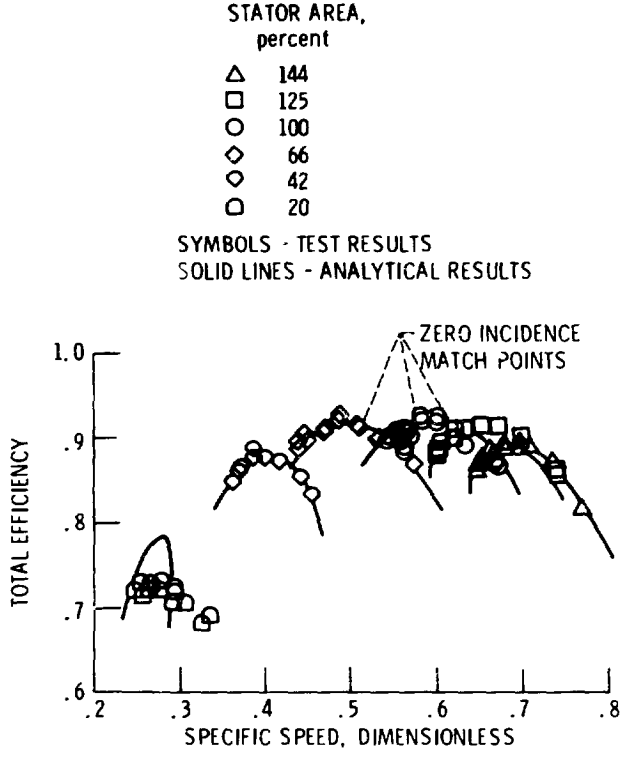

Figure 5. - Turbine total efficiency vs. specific speed (design rotor).

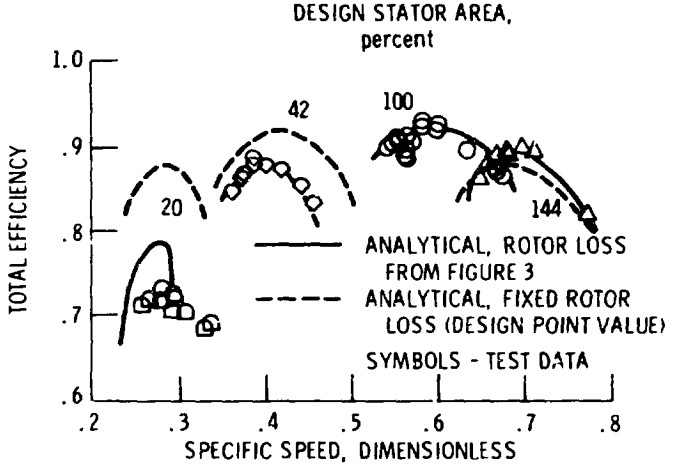

Figure 6. - Loss model comparison (design rotor of (4)).

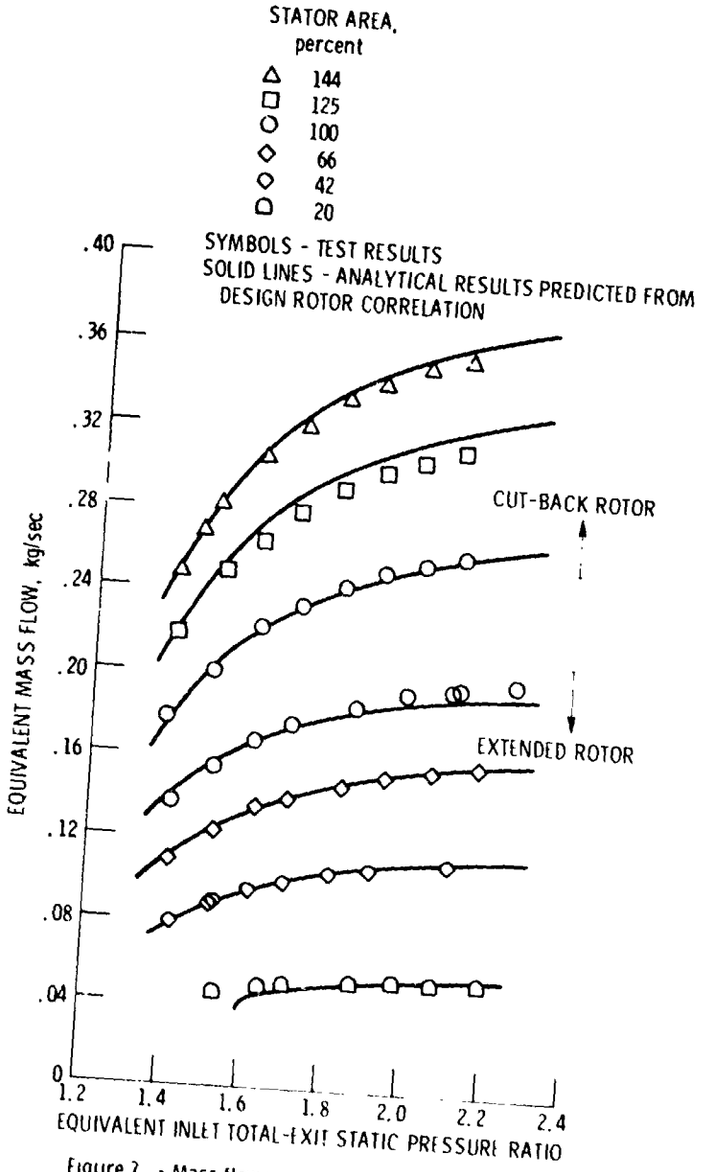

Figure 7. - Mass flow vs. pressure ratio (cut-back and extended rotor).

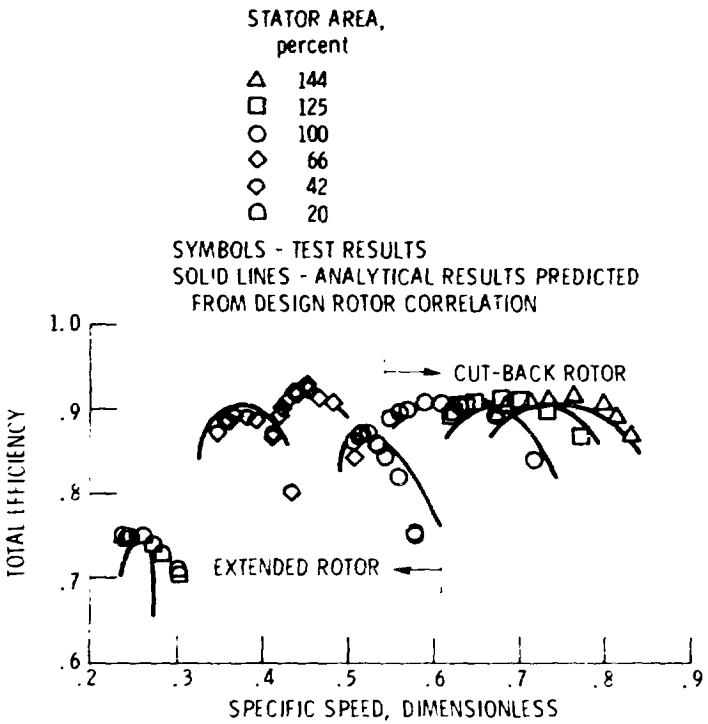

Figure 8. - Turbine total efficiency vs. specific speed (cut-back and extended rotor).

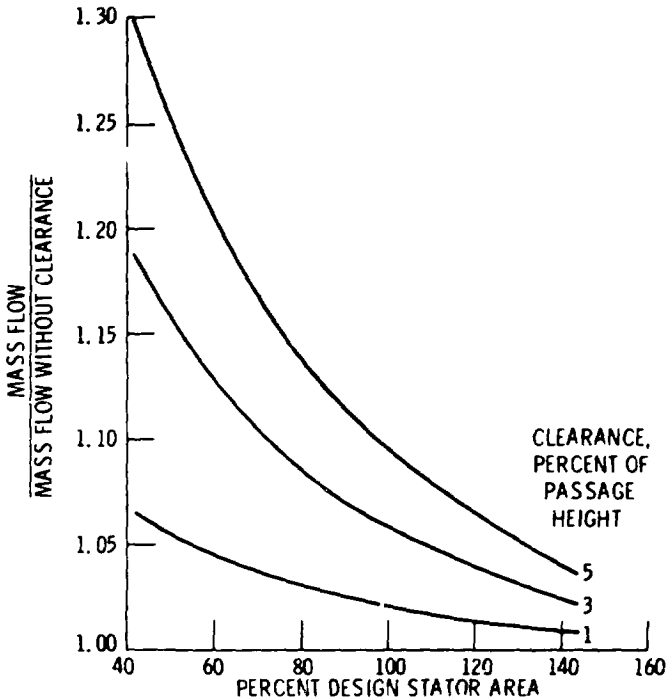

Figure 9. - Effect of stator area and clearance on mass flow (design rotor at constant pressure ratio).

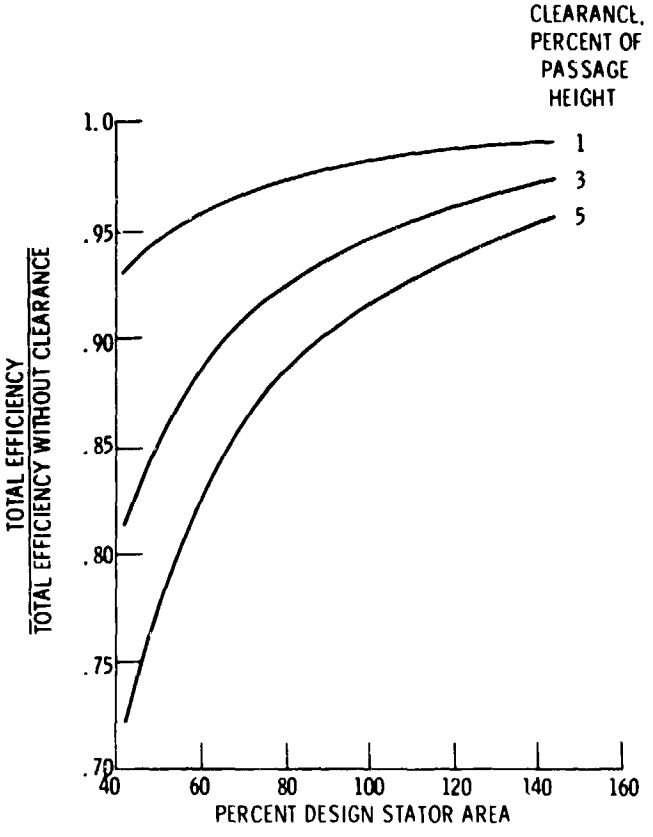

Figure 10. - Effect of stator area and clearance on total efficiency (design rotor at constant pressure ratio).